21 July 2000

ELSEVIER

Chemical Physics Letters 325 (2000) 219–224

CHEMICAL PHYSICS LETTERS

www.elsevier.nl/locate/cplett

# Molecular dynamics of coil–rod–coil molecules depending on their concentrations in polar or non-polar solvent: intra- and intermolecular interactions and charge transfer emissions

In-Wook Hwang, Hyo-Hwi Choi, Byoung-Ki Cho, Myongsoo Lee, Yong-Rok Kim *

*Department of Chemistry, Yonsei University, Shinchon 134, Seoul 120-749, South Korea*

Received 23 February 2000; in final form 19 May 2000

**Abstract**

Concentration-dependent molecular dynamics of long coil–rod–coil molecules at the concentrations of $1 \times 10^{-6}$ M $\sim 1 \times 10^{-4}$ M in polar or non-polar solvent were investigated by steady-state excitation, fluorescence, and picosecond time-resolved fluorescence spectroscopies. The fluorescence spectra of the molecules reveal both characteristics of local excited-state emission and strong intramolecular charge-transfer (ICT) emission. The steady-state excitation spectra and the picosecond time-resolved fluorescence decay profiles in the concentrations of $5 \times 10^{-5}$ M and $1 \times 10^{-4}$ M ascertain hydrophobic rod-to-rod interaction (*J*-aggregation) in methanol solution. The hydrophilic intermolecular interactions (amorphous aggregation) in *n*-hexane are also discussed. © 2000 Elsevier Science B.V. All rights reserved.

## 1. Introduction

It is important to investigate macro- and microstructures to control physical properties of liquid crystal (LC) materials [1,2]. Specific interactions, such as charge-transfer (CT) reaction, hydrogen bonding, hydrophobic interaction, and ionic bonding, etc., are important factors governing physical properties of LC materials. In this study, we have investigated intra- and intermolecular dynamics of relatively long coil–rod–coil ABC triblock molecules which consisted of long rigid hydrophobic biphenyl carboxylate rod and flexible hydrophilic poly(propylene oxide) coil. The coil part of the molecule is also modified into three different chain lengths to investigate the coil length effect as shown in Fig. 1. These molecules were reported to provide a variety of interesting supramolecular structures (crystalline, smetic C, smetic A, cubic, hexagonal columnar, and isotropic, etc.) through LC phase transitions in bulk states [3]. Such structural transitions can occur from the unique inra- and intermolecular interactions among these coil–rod–coil molecules. Therefore, we investigated the detailed intra- and intermolecular interaction dynamics of the molecules by the concentration ($1 \times 10^{-6}$ M $\sim 1 \times 10^{-4}$ M)-dependent studies in polar (methanol) or non-polar (*n*-hexane) solvent. In order to elucidate the molecular dynamics of the coil–rod–coil molecules, especially the intermolecular interactions, we utilized steady-state excitation, fluorescence, and time-resolved fluorescence spectroscopies. From the study, the molecules reveal

* Corresponding author. Fax: +82-2-364-7050; e-mail: yrkim@alchemy.yonsei.ac.kr

0009-2614/00/$ - see front matter 
PII: S0009-2614(00)00625-4

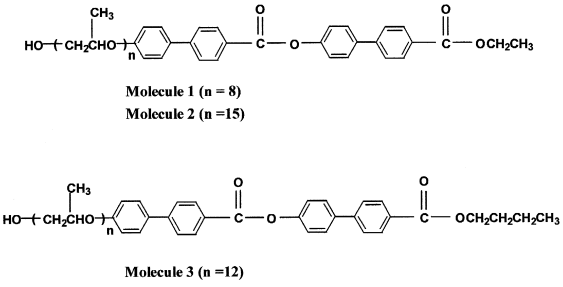


Fig. 1. Coil–rod–coil ABC triblock molecules with poly(propylene oxide) coil lengths of $n = 8$ (Molecule **1**), $n = 15$ (Molecule **2**), and $n = 12$ (Molecule **3**). They were nomenclatured as ethyl 4-[4-[oxypoly(propyleneoxy)propyloxy]-4′-biphenylcarboxyloxy]-4′-biphenylcarboxylate with poly(propylene oxide) coils of $n = 8$ and $n = 15$, and butyl 4-[4-[oxypoly(propyleneoxy)propyloxy]-4′-biphenycarboxyloxy]-4′-biphenylcarboxylate with poly(propylene oxide) coil of $n = 12$.

the strong intramolecular charge transfer (ICT) emission characteristics, and the enhanced intermolecular interaction effect when they are compared with the conventional self-assembling molecules [4]. Hydrophobic rod-to-rod intermolecular interaction (*J*-aggregation) in polar solvent and hydrophilic intermolecular interaction (amorphous aggregation) in non-polar solvent are discussed.

## 2. Experimental

The synthetic procedures of the coil–rod–coil molecules have previously been reported [3]. The coil–rod–coil molecules were prepared in the concentrations of $1 \times 10^{-6}$ M, $5 \times 10^{-6}$ M, $1 \times 10^{-5}$ M, $5 \times 10^{-5}$ M, and $1 \times 10^{-4}$ M in a polar solvent of methanol and in a non-polar one of *n*-hexane. Methanol and *n*-hexane were purchased from Merck Chemical co. (HPLC grade). The steady-state fluorescence spectra were measured by a fluorescence spectrophotometer (Hitachi F-4500) at room temperature. Excitation spectra were measured at the maximum intensity wavelengths of the fluorescence spectra. A picosecond time-correlated single photon counting (TCSPC) system was employed for the time-resolved fluorescence decay measurements. The system was consisted of cavity dumped dual-jet dye laser (700 series, coherent) that was synchronously pumped by Nd-YAG laser (Antares 76-YAG, coherent). The full width at half maximum of the instrumental response function was 67 ps. The fluorescence decays were measured at magic-angle emission polarization and their exponential fittings were performed by least-squares deconvolution fitting method.

## 3. Results and discussion

### *3.1. Steady-state excitation and fluorescence spectra*

The steady-state excitation and fluorescence spectra of the molecules in methanol are shown in Fig. 2. The spectra were represented in the concentrations of (1) $1 \times 10^{-6}$ M, (2) $5 \times 10^{-6}$ M, (3) $1 \times 10^{-5}$ M, (4) $5 \times 10^{-5}$ M, and (5) $1 \times 10^{-4}$ M. The concentrations are described as (1), (2), (3), (4), and (5) in the following contents. The fluorescence spectra of Fig. 2 do not show any spectral changes except for their intensities depending on the concentrations. However, the excitation bands around 300 nm in (1) ~ (3) concentrations split into two bands around 330 and 260 nm in (4) and (5) concentrations. The excitation band splittings in other LC films were reported to be originated from *J*-aggregation of the rod-like mesogens: *J*-aggregates with their transition dipole moments parallel to each other results in the red shifts in their absorptions and the enhancements of the fluorescences [5–7]. In our molecular system, the hydrophobic interaction between the rods in polar environment can induce a *J*-aggregation. Such intermolecular effect occurs in more diluted concentration region of $10^{-4}$ M ~ $10^{-5}$ M in this molecular system than those ($10^{-1}$ M ~ $10^{-3}$ M) in other LC materials [5,8]. This indicates that the intermolecular interaction strength between the molecules is enhanced in this longer coil–rod–coil system than those of the conventional self-assembling molecules. Such *J*-aggregation can be described as an intermolecular ground-state complex formation [8,9]. Fig. 2a–c indicate that the *J*-aggregation dynamics do not depend on the coil length of the molecule and do not show any spectral shifts in the fluorescence spectra. To obtain more detailed information on the fluorescence spectra, we performed picosecond lifetime study of the fluorescence spectra in Fig. 2. The results are discussed in Section 3.2.

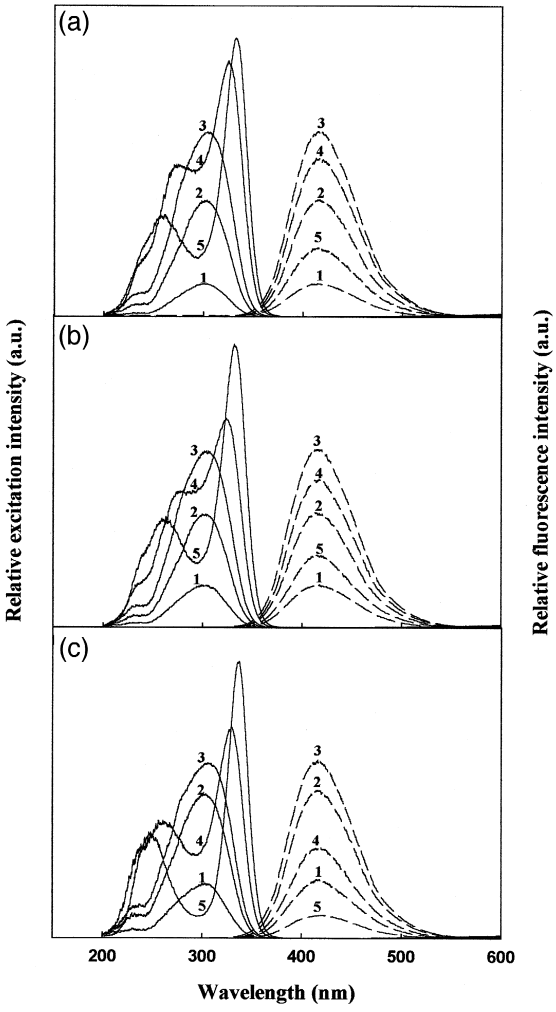


Fig. 2. Steady-state excitation (solid line) and fluorescence (dashed line) spectra of molecule (a) **1**, (b) **2**, and (c) **3** in the concentrations of (1) $1\times10^{-6}$ M, (2) $5\times10^{-6}$ M, (3) $1\times10^{-5}$ M, (4) $5\times10^{-5}$ M, and (5) $1\times10^{-4}$ M in methanol. The excitation wavelength for the fluorescence spectra was 300 nm, and the fixed detection wavelength for the excitation spectra was 420 nm.

Steady-state fluorescence spectra of molecule **1** in *n*-hexane are shown in Fig. 3; the experimental results of molecules **2** and **3** are not represented here since they show similar characteristics to that of molecule **1**. The fluorescence spectrum of Fig. 2a(3) is also represented again as Fig. 3(6) for the comparison. The spectra in Fig. 3 show the large red-shift of 70 nm and the intensity enhancement of 8 times as the solvent environment changes from non-polar (*n*-hexane) to polar (methanol). These results are well agreed with the general characteristics of ICT emissions, i.e., the emissions are stabilized and intensified in polar environments [10,11]. And it indicates that the ICT emission characteristics in these molecules are very strong. The poly(propylene oxide) ether group in the coil part and the ester group in the rod part can be an electron donor and an acceptor, respectively. As a similar ICT dynamics to the molecules, benzene and benzoic acid units are reported to act as an electron donor and acceptor in the biphenyl carboxylic acid molecule [12]. From Fig. 3(4) and (5), we also observed a little red-shift property of the spectra depending on the concentrations in *n*-hexane. Since ICT emission is very sensitive to the polarity around the fluorophore (rod), the red-shifted ICT bands in Fig. 3 imply that the increased concentration in *n*-hexane solution enhances the polarity around the rod [13]. Therefore, it is considered that the hydrophilic poly(propylene oxide) coils of the molecules begin to provide polar environments around the fluorophores (rods) at the concentration of (4) $5\times10^{-5}$ M in non-polar solvent.

### 3.2. Time-resolved fluorescence decay measurements

The fluorescence decay profiles of the molecules in methanol indicate the concentration-dependent

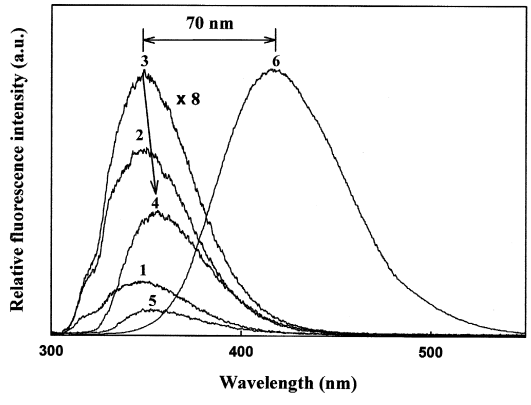


Fig. 3. Steady-state fluorescence spectra of molecule **1** in the concentrations of (1) $1\times10^{-6}$ M, (2) $5\times10^{-6}$ M, (3) $1\times10^{-5}$ M, (4) $5\times10^{-5}$ M, and (5) $1\times10^{-4}$ M in *n*-hexane, and (6) $1\times10^{-5}$ M in methanol. The excitation wavelength was 300 nm.

characteristics as shown in Fig. 4. The decays become faster at the concentration of (4) $5 \times 10^{-5}$ M for all the molecules in methanol. On the other hand, the fluorescence decay profiles of the molecules in *n*-hexane, which are shown in Fig. 5, do not indicate such concentration-dependent properties.

All the fluorescence lifetimes of the molecules revealed one rise and two decay characteristics in both methanol and *n*-hexane as shown in Table 1. Also, the decay profiles (the data are not shown here) from several detection wavelengths indicated that the fast (major) decay components in both methanol and *n*-hexane were responsible for the long wavelength region emissions, and the slow (minor) decay ones were from the short wavelength region emissions. Based on the ICT emission characteristics of the molecules described in Section 3.1, the fast and the slow decay components are suggested to be from the ICT and the local excited-state emission, respectively. It is well known that the energy level of $\pi-\pi^*$ local excited state is higher than that of ICT state [14].

In Fig. 4 and Table 1, the molecules in (1) ~ (3) concentrations of the methanol solution reveal the ICT-state and the local excited-state lifetimes of 510 ~ 532 ps and about 2 ns for molecule **1**, 418 ~ 420 ps and about 2 ns for molecule **2**, and 456 ~ 470 ps and about 2 ns for molecule **3**, respectively. On the other hand, the molecules in (4) and (5) concentrations have the lifetimes of 379 ps and about 2 ns for molecule **1**, 385 ~ 395 ps and about 2 ns for molecule **2**, and 391 ~ 420 ps and about 2 ns for molecule **3**. It indicates that the ICT-state lifetimes of the molecules become faster in (4) $5 \times 10^{-5}$ M and (5) $1 \times 10^{-4}$ M concentrations of the methanol solution. Such faster ICT-state lifetimes are related to the excitation band splitting property in the con-

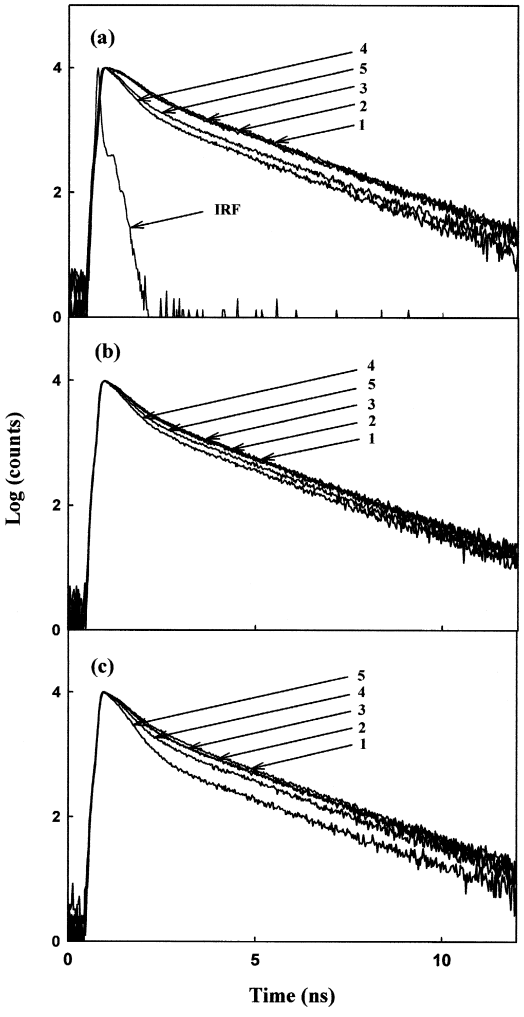


Fig. 4. Time-resolved fluorescence decay profiles of molecule (a) **1**, (b) **2**, and (c) **3** in the concentrations of (1) $1\times10^{-6}$ M, (2) $5\times10^{-6}$ M, (3) $1\times10^{-5}$ M, (4) $5\times10^{-5}$ M, and (5) $1\times10^{-4}$ M in methanol. The decays were measured at the wavelength of 450 nm. IRF represents the instrumental response function of the TCSPC system.

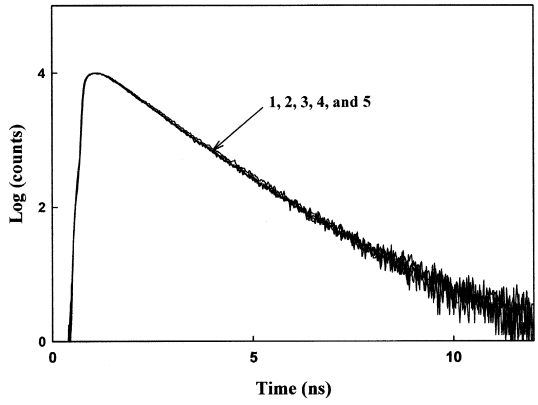


Fig. 5. Time-resolved fluorescence decay profiles of molecule **1** in the concentrations of (1) $1\times10^{-6}$ M, (2) $5\times10^{-6}$ M, (3) $1\times10^{-5}$ M, (4) $5\times10^{-5}$ M, and (5) $1\times10^{-4}$ M in *n*-hexane. The decays were measured at the detection wavelength of 380 nm.

Table 1
Fluorescence lifetimes of the coil–rod–coil molecules in solution

| Solvent | Sample | Concentration | Rise($\tau_1$) (ps) | Decay($\tau_2$) (ps) | Decay($\tau_3$) (ns) | $\chi^2$ |
|---|---|---|---|---|---|---|
| Methanol | Molecule 1 | (1) | 46 | 510 (61%) | 2.013 (39%) | 1.3 |
| | | (2) | 52 | 513 (61%) | 1.989 (39%) | 1.4 |
| | | (3) | 52 | 532 (63%) | 1.997 (37%) | 1.5 |
| | | (4) | 36 | 379 (85%) | 1.974 (15%) | 1.2 |
| | | (5) | 32 | 379 (79%) | 1.963 (21%) | 1.3 |
| | Molecule 2 | (1) | 35 | 420 (71%) | 1.969 (29%) | 1.2 |
| | | (2) | 33 | 418 (74%) | 1.979 (26%) | 1.1 |
| | | (3) | 38 | 419 (72%) | 1.980 (28%) | 1.2 |
| | | (4) | 38 | 385 (84%) | 1.987 (16%) | 1.1 |
| | | (5) | 35 | 395 (79%) | 1.971 (21%) | 1.2 |
| | Molecule 3 | (1) | 65 | 467 (72%) | 2.001 (28%) | 1.1 |
| | | (2) | 60 | 458 (76%) | 1.998 (24%) | 1.3 |
| | | (3) | 49 | 456 (76%) | 1.987 (24%) | 1.4 |
| | | (4) | 52 | 420 (82%) | 1.981 (18%) | 1.5 |
| | | (5) | 40 | 391 (92%) | 2.004 (8%) | 1.3 |
| *n*-Hexane | Molecule 1 [a] | (1) | 113 | 938 (98%) | 2.150 (2%) | 1.2 |
| | | (2) | 112 | 925 (97%) | 2.191 (3%) | 1.3 |
| | | (3) | 109 | 942 (98%) | 2.182 (2%) | 1.2 |
| | | (4) | 120 | 960 (98%) | 2.300 (2%) | 1.2 |
| | | (5) | 123 | 961 (96%) | 1.911 (4%) | 1.3 |

$I(t) = -A_1 e^{-t/\tau_1} + A_2 e^{-t/\tau_2} + A_3 e^{-t/\tau_3}$; $I(t)$, $A$, and $\tau$ are the time-dependent fluorescence intensity, amplitude (noted as the normalized percent in the parentheses), and lifetime, respectively. The concentrations are (1) $1 \times 10^{-6}$ M, (2) $5 \times 10^{-6}$ M, (3) $1 \times 10^{-5}$ M, (4) $5 \times 10^{-5}$ M, and (5) $1 \times 10^{-4}$ M. The excitation wavelength was 300 nm, and the detection wavelengths are 450 nm for the methanol solutions and 380 nm for the *n*-hexane ones.

[a] The experimental results of molecules **2** and **3** in *n*-hexane are not shown here due to the same characteristics with those of molecule **1** in *n*-hexane.

centrations of (4) and (5) of Fig. 2. That is, the faster ICT-state lifetimes are originated from the aforementioned *J*-aggregation between the hydrophobic rods in polar environment. The faster fluorescence lifetimes due to the rod-to-rod interaction was reported in film or solution phase rod-coil molecules [15–17]. The different ICT-state lifetimes of the three molecules at the same concentrations in Table 1 can also be considered due to the coil length effect on the ICT state. Since the rod-to-rod interaction does not occur in the concentrations of (1) ~ (3), the ICT-state lifetimes in these concentrations can be affected by the charge transporting ability from the coils. On the other hand, the lifetimes of the ICT states in (4) and (5) concentrations are to be affected by both the charge transporting ability and the rod-to-rod interaction strength which can bereduced by the steric effect due to the coils.

The fluorescence lifetimes of molecule **1** in *n*-hexane are known to be 925 ~ 961 ps (major) and about 2 ns (minor) from Fig. 5 and Table 1, and they nearly do not depend on the concentrations and the coil lengths of the molecules; the experimental results of molecule **2** and **3** are not represented here since they show the same characteristics as that of molecule **1**. Since the lifetime and the energy level of ICT state can easily be affected by the polarity of the environments [18–20], the fluorescence lifetimes of 925 ~ 961 ps in *n*-hexane solution are considered as the ICT-state lifetimes of molecule **1** in non-polar environment even though they are different from the aforementioned ICT-state lifetimes (379 ~ 532 ps) of molecule **1** in polar (methanol) solutions. From the viewpoint of molecular dynamics, the molecules in *n*-hexane are likely to be affected by the hydrophilic force (intra- or intermolecular interaction) between

the poly(propylene oxide) coils and the ester units in the rods rather than the aforementioned hydrophobic force in the methanol solutions. The strength of this interaction would be larger than that of the hydrophobic one due to their electrostatic property. Therefore, the ICT-state lifetimes of this aggregation do not depend on the concentrations of $1 \times 10^{-6}$ M $\sim 1 \times 10^{-4}$ M and the coil lengths ($n = 8$, 12, and 15) as shown in Fig. 5 and Table 1. This aggregation process can also be non-directional due to their random coil characteristics, and therefore it produces an amorphous aggregated state of the coil–rod–coil molecules.

Finally, the relatively long (109 ~ 123 ps) rise components in *n*-hexane and the short (32 ~ 65 ps) ones in methanol from Figs. 4 and 5, and Table 1 may be due to the excited-state relaxations from the local excited states to the ICT emission states of the molecules. Since the ICT emissions in the *n*-hexane solution occur at the shorter wavelength region than those in the methanol solution as shown in Fig. 3, the amplitude of the excited-state potential barrier between the local excited-state and the ICT emission state is expected to be higher in the *n*-hexane solution than in the methanol solution [12].

## 4. Conclusion

In the study, the fluorescence spectra of the coil–rod–coil molecules revealed the characteristics of the local excited-state emission and the strong ICT emission, which is due to the charge transfer from the ether moiety to the ester in the molecule. In the concentration-dependent study of the methanol solution, the faster ICT-state lifetimes and the excitation band splittings in the concentrations of (4) $5 \times 10^{-5}$ M and (5) $1 \times 10^{-4}$ M indicated the *J*-aggregation formation by the hydrophobic rod-to-rod interaction in the polar environment. This concentration region is the relatively dilute condition to form a *J*-aggregation, comparing with those of other conventional LC molecules. The fluorescence decay profiles of the coil–rod–coil molecules in *n*-hexane consistently indicate about 950 ps (major) and 2 ns (minor) lifetimes, which do not depend on the concentrations and the coil lengths of the molecules. These results elucidate non-directional amorphous aggregations of the coil–rod–coil molecules in *n*-hexane. Such molecular dynamic information of the coil–rod–coil molecules in solution can be essential in order to understand the detailed LC phase transitions in bulk states. The research in bulk state is presently in progress in this group.

## Acknowledgements

This research was financially supported by CRM-KOSEF Grant 1998G0102, South Korea.

## References

[1] A. Blumstein, Polymeric Liquid Crystals, Plenum Press, New York, 1985.
[2] S.A. Jenekhe, X.L. Chen, Science 279 (1998) 1903.
[3] M. Lee, B.-K. Cho, H. Kim, J.-Y. Yoon, W.-C. Zin, J. Am. Chem. Soc. 120 (1998) 9168.
[4] Y. Hayashi, K. Ichimura, Langmuir 12 (1996) 831.
[5] T. Imamura, K. Watanabe, Y. Tsuboi, H. Miyasaka, A. Itaya, Thin Solid Films 338 (1999) 243.
[6] F. Rotermund, R. Weigand, A. Penzkofer, Chem. Phys. 220 (1997) 385.
[7] X.L. Chen, S.A. Jenekhe, Langmuir 15 (1999) 8007.
[8] M. Sone, T. Wada, B.R. Harkness, J. Watanabe, H. Takahashi, H.W. Huang, T. Yamashita, K. Horie, Macromolecules 31 (1998) 8865.
[9] H.W. Huang, K. Horie, T. Yamashita, S. Machida, M. Sone, M. Tokita, J. Watanabe, Y. Maeda, Macromolecules 29 (1996) 3485.
[10] W. Rettig, Angew. Chem. Int. Ed. Engl. 25 (1986) 971.
[11] K. Bhattacharyya, M. Chowdhurry, Chem. Rev. 93 (1993) 507.
[12] M. Yoon, D.W. Cho, J.Y. Lee, Bull. Korean Chem. Soc. 13 (1992) 613.
[13] G. Saroja, A. Samanta, J. Chem. Soc. Faraday Trans. 94 (1998) 3141.
[14] I.-W. Hwang, N.W. Song, D. Kim, Y.T. Park, Y.-R. Kim, J. Polym. Sci. Part B: Polym. Phys. 37 (1999) 2901.
[15] J.A. Osaheni, S.A. Jenekhe, J. Am. Chem. Soc. 117 (1995) 7389.
[16] D. Oelkrug, A. Tompert, J. Gierschner, H.-J. Egelhaaf, M. Hanack, M. Hohloch, E. Steinhuber, J. Phys. Chem. B 102 (1998) 1902.
[17] S.A. Jenekhe, X.L. Chen, Science 283 (1999) 372.
[18] B. Strehmel, A.M. Sarker, J.H. Malpert, V. Strehmel, H. Seifert, D.C. Neckers, J. Am. Chem. Soc. 121 (1999) 1226.
[19] J.D. Simon, S.-G. Su, J. Phys. Chem. 92 (1988) 2393.
[20] G. Saroja, A. Samanta, J. Chem. Soc. Faraday Trans. 92 (1996) 2697.